



Ground Vibration Test and Dynamic Response of Horseshoe-shaped Pipeline During Tunnel Blasting Excavation in Pebbly Sandy Soil

Xiaoming Guan · Xuchun Wang · Zhen Zhu  · Liang Zhang · Hongxian Fu

Received: 18 December 2019 / Accepted: 21 February 2020 / Published online: 27 February 2020
© Springer Nature Switzerland AG 2020

Abstract In order to ensure the safety of horseshoe-shaped pipeline during tunnel blasting excavation, the vibration test and dynamic response of horseshoe-shaped pipeline were investigated. The velocity and frequency of tunnel blasting vibration were analyzed. Sodev's empirical formula was used for regression analysis of the velocity of blasting vibration. 3D numerical model of a horseshoe-shaped pipelines was established with ALE algorithm using ANSYS/LS-DYNA. The propagation law of a blasting seismic wave was analyzed, and the transverse and longitudinal vibration response characteristics of pipelines under tunnel blasting vibration were studied. The velocity of the pipeline increases gradually and the

frequency tends to decrease with the decrease of the distance away from the explosion source center under the same charge. The principal frequency of vibration in the Z direction is mainly distributed from 50 to 80 Hz, which is difficult to generate resonance with the pipelines. The maximum relative error between the simulated and measured velocity of X, Y and Z directions was 8.2%. It was reliable to study the dynamic response of pipelines under blasting vibration based on this numerical model. The blasting seismic wave first reached the bottom of the pipeline right above the explosive. Subsequently, seismic waves propagated along the transverse and the longitudinal axes of the pipeline, and the pressure on the pipeline increased gradually. And when it attenuated completely in the soil, the pipeline stopped its response. The peak value of tensile stress of each element of the vault is the largest. However, the velocity of the bottom plate and the arch roof of pipeline are the largest. The peak values of velocity and tensile stress exist in 0 to 4 m away from the explosion source, and gradually decrease as the distance away from the explosion source increases.

X. Guan · X. Wang · Z. Zhu (✉)
School of Civil Engineering, Qingdao University of
Technology, Qingdao 266033, China
e-mail: zhuzhen88@foxmail.com

X. Guan
e-mail: guanxiaoming@qut.edu.cn

X. Wang
e-mail: xcwang2008@foxmail.com

L. Zhang
School of Civil Engineering, Southwest Jiaotong
University, Chengdu 610031, China
e-mail: zhangliang@qut.edu.cn

H. Fu
School of Civil Engineering, Beijing Jiaotong University,
Beijing 100044, China
e-mail: fhxllj@163.com

Keywords Horseshoe-shaped pipeline · Tunnel blasting · Numerical simulation · ALE algorithm · Vibration response

1 Introduction

Underground municipal pipelines are the city's arteries and lifelines. The number of tunneling projects is rapid increasing year by year. The dynamic response, damage mechanism, and safety of an underground pipeline at a close distance to blasting excavation are major theoretical and technical problems in tunnel construction. However, due to unclear damage mechanisms of pipelines subjected to blasting vibration and a lack of effective blasting vibration monitoring methods and safety standards, it is easy to cause major construction accidents. Therefore, it is necessary to thoroughly evaluate the dynamic responses of the pipeline subjected to tunnel blasting vibrations to guarantee the safety of the pipeline during construction.

The blasting vibration on pipelines have been studied by a number of researchers using field and laboratory experiments and numerical simulation methods. De et al. (2016) found that a protective device made of polyurethane material was effective to reduce the damage caused by a blasting load. Linear and nonlinear dynamic responses of underground pipelines under explosions in soil were also studied by Mane and Shete (2017). Formulae for calculating the peak strain of seamless steel pipe based on the distance from the detonation center and the charge were obtained by Zhong et al. (2018). Zhang et al. (2017) found that the axial and circumferential strain of underground pipeline is related to the surface synthetic peak vibration velocity in an exponential function. Liu (2012) analyzed the interaction and failure mechanism between an underground circular cast iron structure and the soil layer under an internal explosion using ABAQUS. Mokhtari and Nia (2015, 2016) analyzed an X65 steel tube using ABAQUS and found that the deformation and maximum equivalent strain decreased as the operating pressure increased and the diameter to thickness ratio decreased. Zhang et al. (2013) simulated and analyzed the deformation and failure modes of an underground pipeline under the impact of an explosion in soil using AUTODYN. Zhang et al. (2016) analyzed the effects of internal pressure, TNT size, wall thickness, and buried depth on the stress and strain of a pipeline using LS-DYNA with the ALE algorithm. Blasting vibration characteristics and safety standard of a circular pipeline passed down by tunnel in a short distance were analyzed

(Guan et al. 2019). In order to assess and predict the influence of blasting vibration, a PPV prediction model of gas pipeline under metro tunnel excavation blasting was proposed (Jiang et al. 2018). Besides, the physics and mechanics properties of rock around the pipeline also affect the response of pipe subjected to blasting. Continuum analysis of the structurally controlled displacements for large-scale underground caverns in bedded rock masses was analyzed (Li et al. 2020). Energy evolution characteristics of coal specimens with preformed holes under uniaxial compression was studied (Wu et al. 2020). Multi-scale effect of acoustic emission characteristics of 3D rock damage was investigated (Liu et al. 2019). However, the monitoring method and safety standard of the pipeline under tunnel blasting vibration need to be further studied.

The research on velocity and frequency of blasting vibration and stress response of a tunnel passing close to reinforced concrete pipelines is not systematic. In this paper, based on the blasting construction of a shallow buried big-span tunnel passing underneath water pipelines, the blasting vibration test was carried out, and the blasting vibration velocity and frequency were analyzed. Sodev's empirical formula was used for regression analysis of blasting vibration velocity. Three-dimensional numerical models of a horseshoe-shaped pipelines was established with ALE algorithm using ANSYS/LS-DYNA. The propagation law of a blasting seismic wave was analyzed, and the transverse and longitudinal vibration response characteristics of pipelines under tunnel blasting vibration were studied.

2 The Information of Tunnel and Pipeline and Blasting Vibration Test

2.1 The Tunnel and Pipeline

The total length of a highway tunnel is about 1700 m. Most of the tunnels are shallow buried with a large span. This tunnel passes through more than 13 municipal pipelines at a short distance. Among them, there is a horseshoe-shaped pipeline (Fig. 1). The minimum clear distance is only 13.60 m, which is smaller than the diameter (16.8 m) of the tunnel. The tunnel was constructed using the method of drilling and blasting of up-middle-down short benches. The

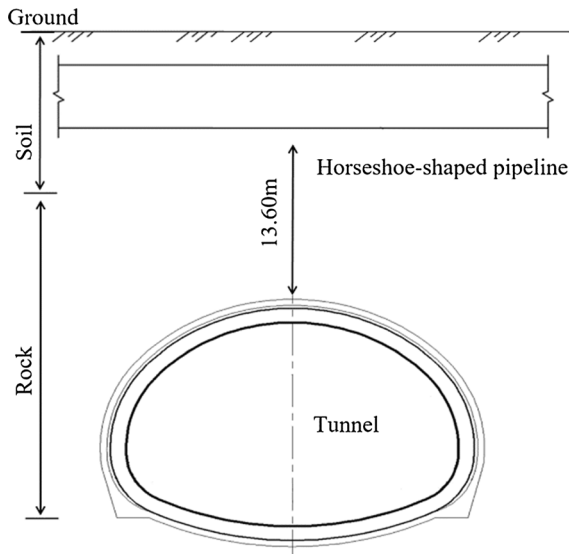


Fig. 1 Position relationship between tunnel and horseshoe-shaped pipeline

arrangement of the blast holes and the design of delay detonators of the blast holes of Part I and Part II in the upper bench were given in Fig. 2.

The horseshoe-shaped water supply pipeline was built in 1990, which is unpressurized water pipeline. The pipe has dimensions of 3.6 m (width) × 4.68 m (height), as shown in Fig. 3. The side and arch wall of pipeline are made of C30 reinforced concrete with a thickness of 40 cm, and above the pipeline is about 1 m thick soil. The rock under the pipeline of the tunnel is pebbly sandy soil.

2.2 Blasting Vibration Test and Result Analysis

In this paper, the blasting vibration testing system was composed of a blasting monitor and a 3D velocity

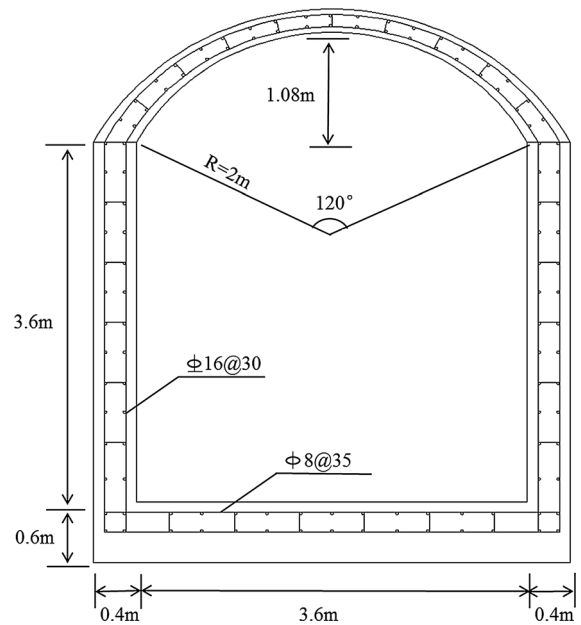


Fig. 3 Structural dimensions of horseshoe-shaped pipeline

sensor, which was used to collect the blasting vibration data when tunnel blasting went through the pipeline. The system was shown in Fig. 4. Since the horseshoe pipeline is about 1.0 m away from the ground, blasting vibration test is conducted on the ground to study the propagation characteristics of blasting seismic wave. The test data of blasting vibration were shown in the Table 1.

It can be seen that the vibration velocity of the pipeline increases gradually with the decrease of the distance from the explosion source center under the same charge. The principal frequency of vibration in the Z direction is mainly distributed from 50 to 80 Hz. And the frequency tends to decrease with the decrease of distance from the center of explosion source. At the

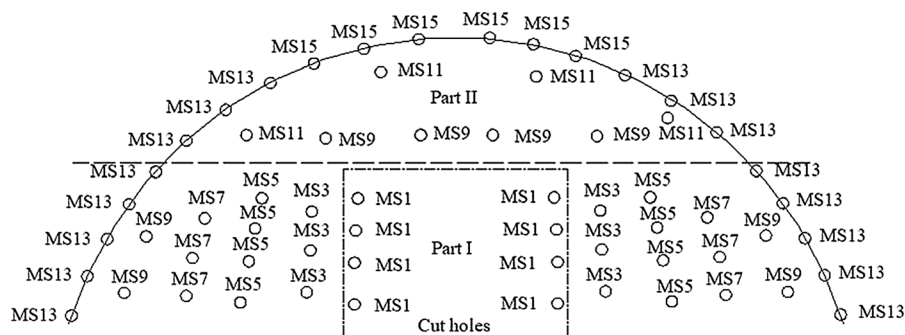


Fig. 2 The blasting holes arrangement of top bench

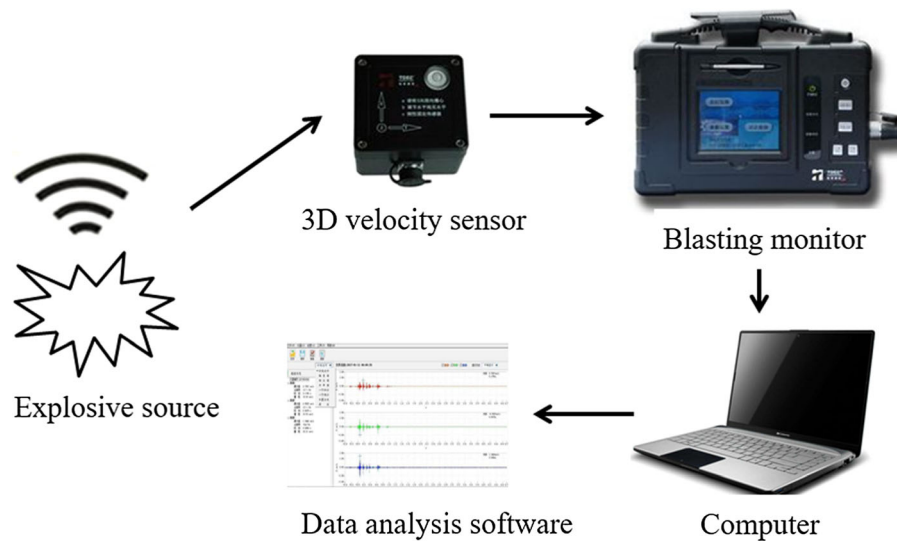


Fig. 4 The blasting vibration testing system

Table 1 The test data of blasting vibration

No	Horizontal distance from excavation face to pipeline (m)	Distance away from explosive source (m)	Charge of cut holes (kg)	Peak velocity (cm/s)			Frequency (Hz)
				X	Y	Z	Z
1	40	41.94	7.2	0.212	0.232	0.501	71.2
2	38	40.03	7.2	0.254	0.167	0.547	82.2
3	36	38.14	7.2	0.337	0.208	0.611	77.2
4	33	35.32	7.2	0.408	0.374	0.694	63.5
5	31	33.42	7.2	0.343	0.348	0.738	61.4
6	30	32.42	5.6	0.396	0.194	0.665	65.1
7	29	31.62	5.6	0.321	0.173	0.725	78.4
8	28	30.7	5.6	0.373	0.292	0.744	85.5
9	25	27.99	3.6	0.210	0.225	0.557	73.2
10	24	27.10	3.6	0.223	0.228	0.582	74.6
11	22	25.35	3.2	0.458	0.378	0.679	80.8
12	21	24.49	3.2	0.365	0.324	0.718	65.6
13	20	23.68	3.2	0.443	0.358	0.734	53.0
14	18	21.87	3.2	0.521	0.483	0.823	62.6
15	15	19.58	3.2	0.537	0.583	1.184	66.1

same time, the natural vibration frequency of most underground pipelines is from 4 to 10 Hz, indicating that the ground vibration caused by tunnel blasting is difficult to generate resonance with the pipelines, which is conducive to the safe operation of underground pipelines (Xu et al. 2003).

In practical engineering, Sodev's empirical formula is often used to determine the vibration velocity of blasting and is mostly used for regression analysis of blasting vibration velocity (Zhang et al. 2008). The Sodev's empirical formula is as follows.

$$V = k \left(\frac{Q^{1/3}}{R} \right)^\alpha \tag{1}$$

where V is the particle velocity (cm/s); Q is the charge (kg); R is the monitoring point from the blasting source (m); k is the coefficient related to the rock medium and blasting conditions; α is the attenuation coefficient of vibration.

The peak vibration velocity in the Z direction of the measuring point is the largest, therefore the regression analysis of the peak vibration velocity in the Z direction of the measuring point in Table 1 is carried out. The result was given in Fig. 5. The Sodev’s empirical formula of V_z is shown in (2), where, V_z is the velocity of Z direction (cm/s); Q is the charge (kg); and R is the distance from the test points to the explosive source (m). This formula can be used to study the blasting attenuation law of tunnel blasting through water supply pipeline and provide guidance for subsequent tunnel blasting construction.

$$V_z = 67.71 \left(\frac{\sqrt[3]{Q}}{R} \right)^{1.42} \tag{2}$$

3 Numerical Model and Simulation Method

3.1 3D Model

A symmetrical model was built by taking the YOZ plane as the symmetric plane. The size of the 3D model is 30 m (length) × 18 m (width) × 30 m

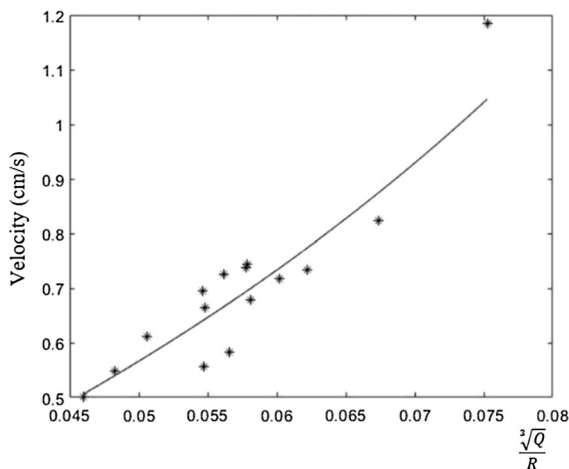


Fig. 5 Regression analysis curve of blasting vibration velocity

(height), the unit size is controlled at about 35 cm, given in Fig. 6. The equivalent diameter method was used to simplify multiple cut holes into one hole, because the distance between the cut holes is much smaller than the distance between the tunnel and the pipeline (Lin et al. 2010). Surface automatic restraint is adopted between the soil layer and the pipeline, and a common joint is adopted between the soil layer and the rock stratum. Symmetric constraints are imposed on the symmetric surface of the model. The top surface is defined as a free surface and the other surfaces are defined as a non-reflective boundary (Jiang et al. 2005). The selection of units, the direction of pipeline length and the steel element have been given in Fig. 7.

3.2 Material Model and Parameters

3.2.1 Air

The air is described by MAT_NULL material model and EOS_LINEAR_POLYNOMIAL equation of state. The pressure is as follows (Hallquist 2015):

$$P = C_0 + C_1\mu + C_2\mu^2 + C_3\mu^3 + (C_4\mu + C_5\mu + C_6\mu^2)E_0 \tag{3}$$

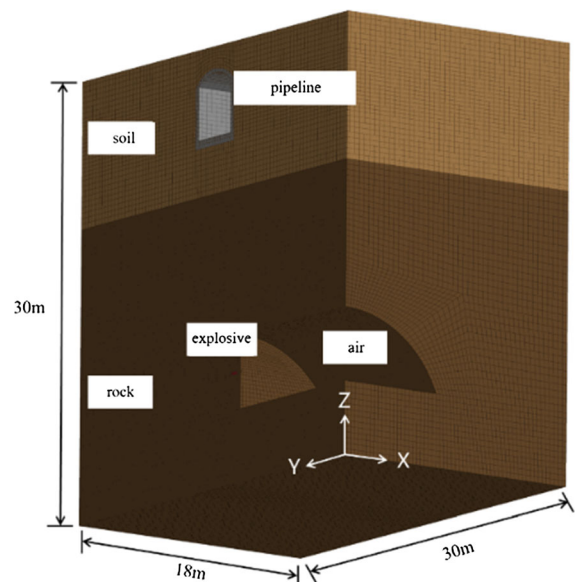


Fig. 6 The finite element model and meshing

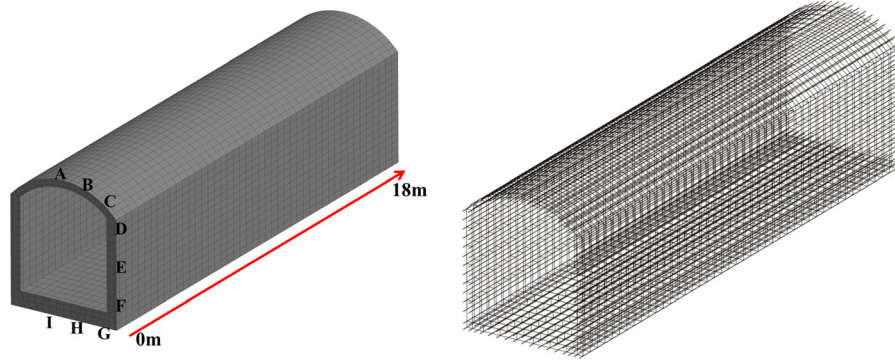


Fig. 7 Concrete and steel element

where $\mu = \rho/\rho_0 - 1$, ρ is the current density, ρ_0 is the initial density; E_0 is the initial internal energy per volume; $C_0, C_1, C_2, C_3, C_4, C_5$ and C_6 are constants, V_0 is the initial volume. The air material parameters are shown in Table 2 (Ma et al. 2011).

3.2.2 Explosive

The explosive charge weight was modelled using (MAT_HIGH_EXPLOSIVE_BURN). The Jones-Wilkens-Lee (JWL) Equation of State (EOS) is used to calculate the detonation pressure (Hallquist 2015):

$$P = A \left(1 - \frac{\omega}{R_1 V} \right) e^{-VR_1} + B \left(1 - \frac{\omega}{R_2 V} \right) e^{-VR_2} + \frac{\omega E_0}{V} \quad (4)$$

where E is the internal energy per unit volume, V is the relative volume of the explosive product, and A, B, R_1, R_2 , and ω are the equation constants for the explosive, D is the detonation velocity. Table 3 gives the material parameters of No.2 rock emulsion explosive (Liu et al. 2012).

3.2.3 Rock Stratum and Soil

The rock stratum was modeled using MAT_PLASTIC_KINEMATIC material model (Hallquist 2015). The specific parameters are shown in Table 4. E is the

elasticity modulus, f_y is the yield strength, E_{tan} is the tangent modulus, β is the hardening parameter.

The soil layer is modeled using MAT_FHWA_SOIL model, and is suitable for simulating soil materials in explosive problems (Jayasinghe et al. 2013; Qin et al. 2019). Most of the soil layers in the pipeline section below the tunnel are gravel sand, and its material parameters are shown in Table 5 (Lewis 2004). G_s is the specific gravity of soil grain, K is the bulk modulus, G is the shear modulus, c is the cohesion, ϕ is the internal friction angle, and W is the moisture content.

3.2.4 Concrete and Steel

The strength of underground pipeline concrete is C30, which is simulated by the MAT_72R3 model. The parameters of C30 concrete are shown in Table 6 (Malvar and Simons 1996). The longitudinal reinforcement of underground pipeline is HRB335 with a tensile strength of 335 MPa; the stirrups are HPB235 with a tensile strength of 235 MPa. The reinforcement is modeled using the MAT_PLASTIC_KINEMATIC material model, and the influence of strain rate effect on yield strength is considered according to the COWPER_SYMONDS model. The material parameters are shown in Table 7 (Zhang et al. 2009). ν is the Poisson's ratio, C and P are strain rate coefficients,

Table 2 Parameters of air

ρ (kg/m ³)	C_0	C_1	C_2	C_3	C_4	C_5	C_6	E_0 (MPa)	V_0
1.29	- 0.1	0	0	0	0.4	0.4	0	0.25	1

Table 3 Parameters of explosive

Density (kg/m ³)	<i>D</i> (m/s)	<i>P</i> _{cj} (GPa)	<i>A</i> (GPa)	<i>B</i> (GPa)	<i>R</i> ₁	<i>R</i> ₂	<i>ω</i>	<i>E</i> ₀ (MPa)
1200	4000	7.4	214.4	0.182	4.2	0.9	0.15	4.192

Table 4 Parameters of rock

Density (kg/m ³)	<i>E</i> (GPa)	Poisson’s ratio	<i>f</i> _y (MPa)	<i>E</i> _{tan} (GPa)	<i>β</i>
2400	3.4	0.18	30	0.5	0.5

Table 5 Parameters of soil

Density (kg/m ³)	<i>G</i> _s	<i>K</i> (MPa)	<i>G</i> (MPa)	<i>c</i> (MPa)	<i>φ</i> (rad)	<i>W</i> (%)
2200	2.65	115	60	6.2×10^{-5}	0.61	0.25

Table 6 Parameters of concrete

Density (kg/m ³)	<i>A</i> ₀	RSIZE	UCF
2300	– 30	0.3940	1.450×10^7

which are used to define the dynamic increase coefficient of the reinforcement, and *F*_s is the failure strain.

3.3 ALE Algorithm

In order to avoid the mesh serious distortion caused by excessive element deformation in the calculation process, ALE algorithm was selected for tunnel blasting simulation. Compared with Lagrange algorithm, ALE algorithm can effectively deal with large deformation problems, which can also provide a clearer definition of the interface of material flow than Euler algorithm (Li et al. 2008). In this paper,

explosive and air are divided into Euler grid, and ALE_MULTI-MATERIAL_GROUP keyword was used to bind them in the same element algorithm. The rock, soil and pipeline were divided into Lagrange grid, and fluid–solid coupling was realized between Lagrange grid and Euler grid by defining CONSTRAINED_LAGRANGE_IN_SOLID (Koneshwaran 2014).

3.4 Model Verification

In order to verify that the numerical simulation results were reasonable, the velocity of the ground vibration during tunnel blasting construction was measured using NUBOX-8016 monitor and compared with the values obtained by numerical simulation. The charge of explosive is 3.2 kg, and the distance from explosive source is 16.80 m. The comparison of particle vibration velocity of monitoring points was given in Table 8. The waveform comparison figure of the measured and simulated vibration on the ground

Table 7 Parameters of steel

Steel type	Density (kg/m ³)	<i>E</i> (GPa)	<i>ν</i>	<i>f</i> _y (MPa)	<i>E</i> _{tan} (GPa)	<i>β</i>	<i>C</i>	<i>P</i>	<i>F</i> _s
Longitudinal bar	7850	206	0.3	335	1	0	40.5	5	0.12
Stirrup	7850	206	0.3	235	1	0	40.5	5	0.12

Table 8 Comparison of particle vibration velocity of monitoring points

Direction	Velocity (cm/s)		Error (%)
	Simulation data	Measuring data	
X	0.67	0.73	− 8.2
Y	1.60	1.51	5.9
Z	2.16	2.27	− 4.8

surface was given in Fig. 8. It can be found that the maximum relative error between the simulated vibration velocity and the measured peak velocity of X, Y and Z directions was 8.2%. Therefore, it was reliable to study the dynamic response of underground pipelines under blasting vibration based on the numerical calculation model.

4 Simulation Result Analysis

4.1 The Blasting Seismic Wave Propagating Rules

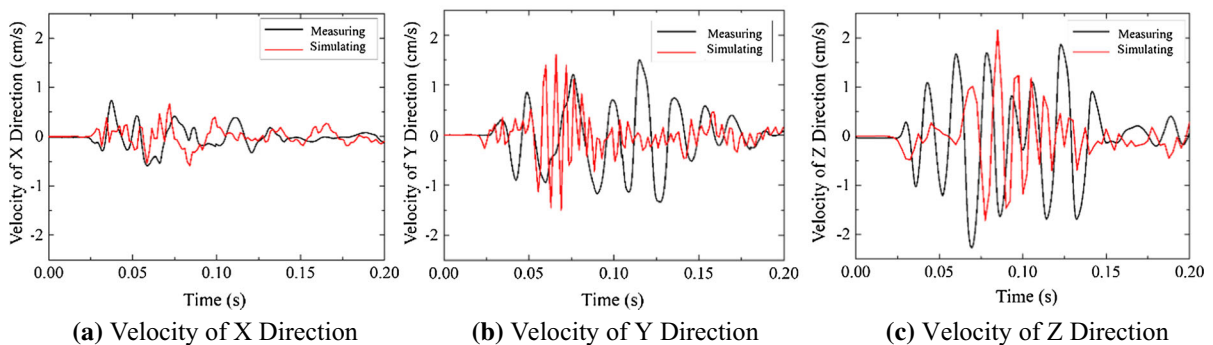
The propagation of blasting waves in rocks media at different times was given in Fig. 9. After the detonation of the column charge, the blasting seismic wave propagates in the form of spherical waves through the rock stratum, shown in Fig. 9a. The area of surface wave increases and the peak pressure decreases with the propagation of the blasting wave. The blasting seismic wave propagates to the boundary of rock and soil at $t = 10$ ms, shown in Fig. 9b. As shown in Fig. 9c, at the time of $t = 15$ ms, the blasting seismic

wave propagates to the lower surface of the pipeline. It can be seen from Fig. 9d that seismic waves are reflected and transmitted at the junction of rock and soil. Some of them are reflected back to the rock stratum and propagate in the rock, while others are transmitted through the interface in the soil layer.

The propagation of blasting seismic wave on pipeline at different time was shown in Fig. 10. The blasting seismic wave first reached the bottom of the pipeline right above the explosive, shown in Fig. 10a. Subsequently, seismic waves propagated along the transverse and the longitudinal axes of the pipeline, and the pressure on the pipeline increased gradually, shown in Fig. 10b, c. At about the time of $t = 22.5$ ms (Fig. 10d), the entire pipeline was subjected to blasting seismic waves. As time passed away, the peak pressure of blasting seismic wave decreased gradually, and when it attenuated completely in the soil, the pipeline stopped its response.

4.2 Dynamic Response of Pipeline

The vibration response of underground structures is mainly analyzed by the peak vibration velocity and tensile stress of the structure (Guan et al. 2017). The section above the explosion center was first selected to analyze the peak velocity and tensile stress of the element at different parts of the section. Then, taking this cross section as the starting point (0 m), the variation law of the peak vibration velocity and the peak tensile stress of each part of the pipeline along the pipeline longitudinal direction was studied. The selection of each part element and the pipeline longitudinal direction were marked in Fig. 7.

**Fig. 8** Time history of velocity at monitoring point

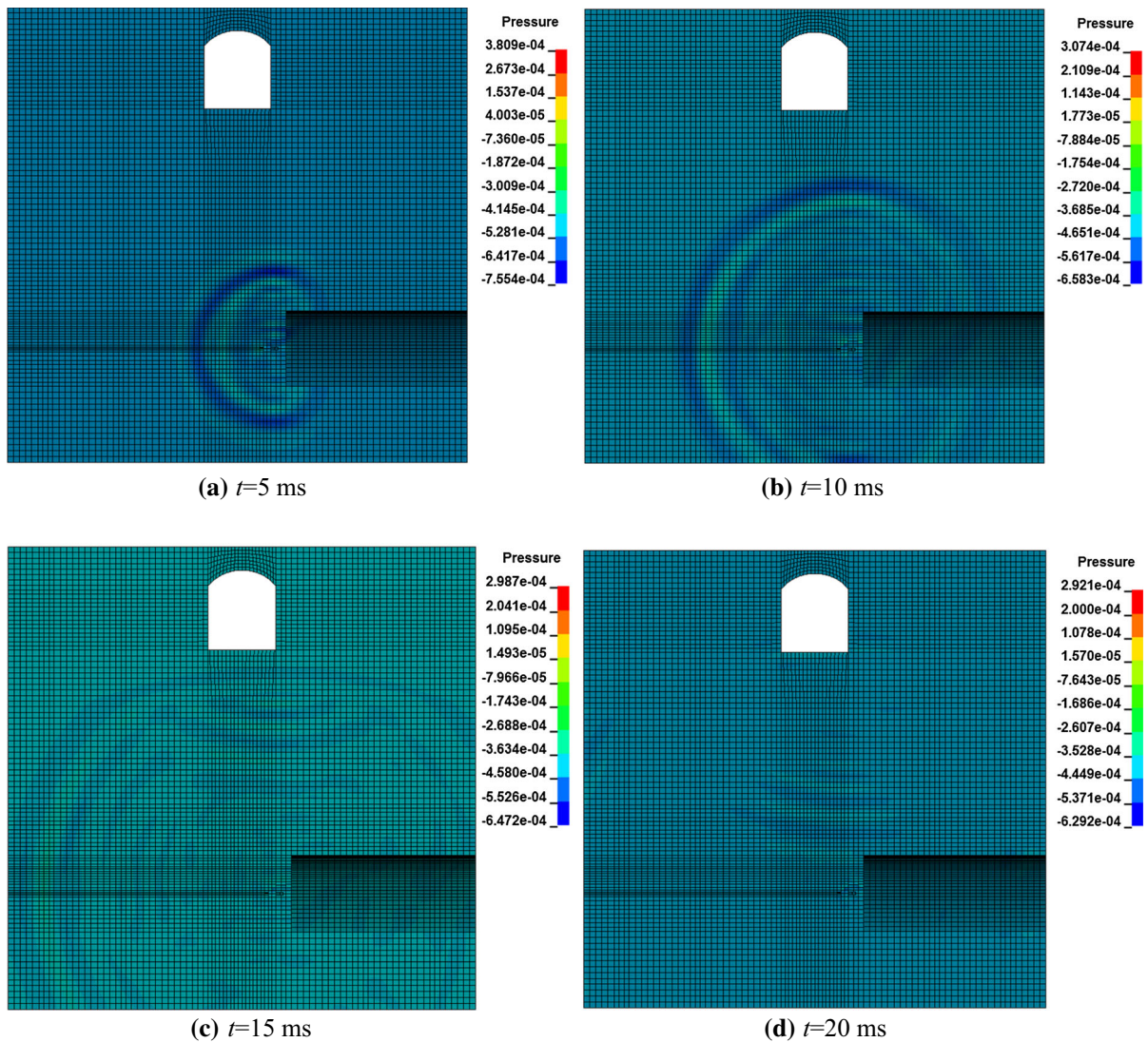


Fig. 9 Pressure contours in the rock and soil at different times (unit: 10^2 GPa)

The variation law of peak tensile stress at different sections of different elements of the pipe in case 9 was shown in Fig. 11. It can be seen that there is a big difference between the peak value of tensile stress in each section of the horseshoe pipe just above the explosion center. The peak value of tensile stress of each element of the vault is the largest, followed by that of the bottom plate, and that of the side wall is the smallest. Among them, the peak tensile stress of the element at vault C was the largest, about 0.57 Mpa, followed by was the element at vault A, about 0.45 Mpa. The largest value element of the bottom plate was at I, about 0.31 Mpa. The peak tensile stress of

each element of the sidewall were not different from each other, neither of which exceeded 0.2 Mpa.

The variation law of peak velocity of Z direction at different sections of different elements of the pipe in case 9 was shown in Fig. 12. It can be seen that there is a big difference between the peak value of velocity in each section of the horseshoe pipe just above the explosion center. The bottom plate and the arch roof of the pipeline have the maximum vibration velocity, and the maximum value of the peak vibration velocity occurs at the I of the bottom plate, about 3.17 cm/s, followed by was the C of the arch, about 3.08 cm/s,

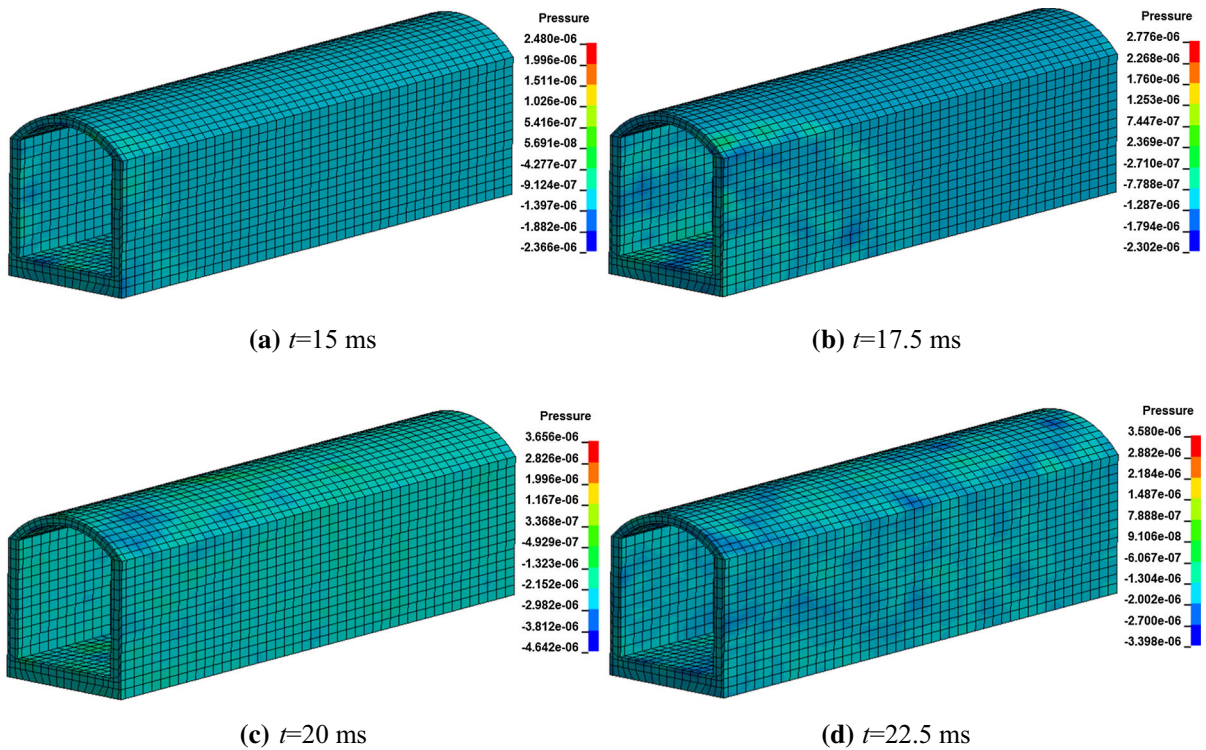


Fig. 10 Pressure contours on the horseshoe-shaped pipeline at different times (unit: 10^2 GPa)

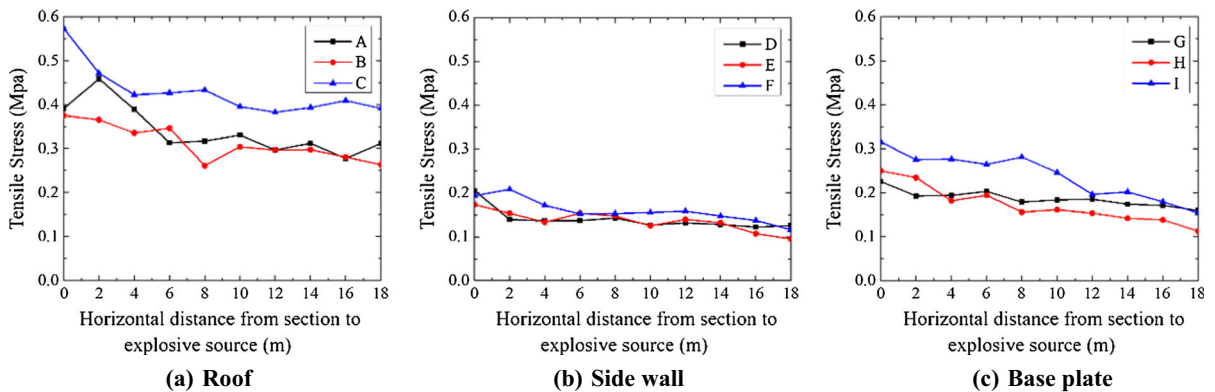


Fig. 11 Comparison of peak tensile stress along the length direction

and the rest of the vibration velocity peaks were all less than 2.0 cm/s.

The peak value of vibration velocity and the peak value of tensile stress of each part of the horseshoe pipeline change in the longitudinal direction in a relatively consistent way. The peak values occur at 0 to 4 m away from the explosion source, and gradually decrease as the distance from the explosion source increases.

5 Conclusions

1. The velocity of the pipeline increases gradually with the decrease of the distance away from the explosion source center under the same charge. The principal frequency of vibration in the Z direction is mainly distributed from 50 Hz to 80 Hz. And the frequency tends to decrease with the

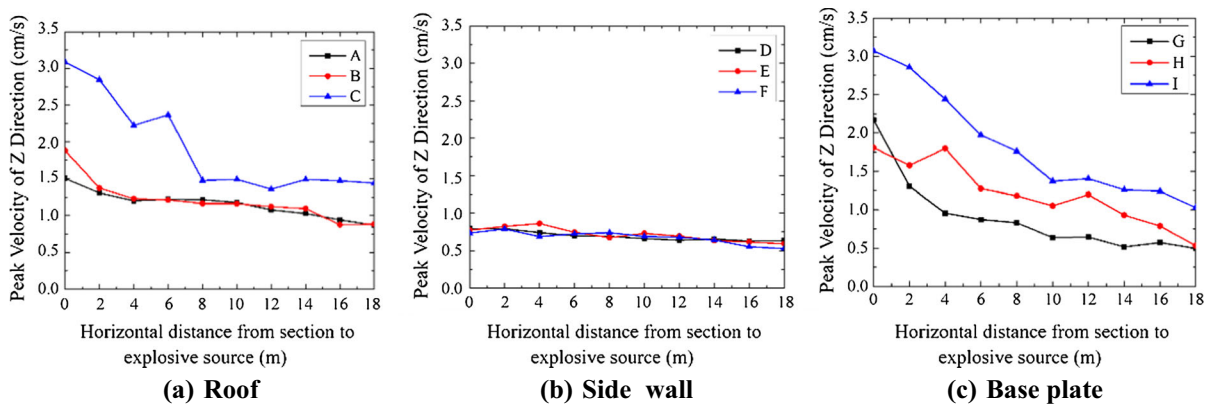


Fig. 12 Comparison of peak tensile stress along the length direction

decrease of distance away from the center of explosion source. The ground vibration caused by tunnel blasting is difficult to generate resonance with the pipelines, because the natural frequency of most underground pipelines is from 4 Hz to 10 Hz.

2. The maximum relative error between the simulated vibration velocity and the measured peak velocity of X, Y and Z directions was 8.2%. It was reliable to study the dynamic response of underground pipelines under blasting vibration based on the numerical model.
3. The blasting seismic wave first reached the bottom of the pipeline right above the explosive. Subsequently, seismic waves propagated along the transverse and the longitudinal axes of the pipeline, and the pressure on the pipeline increased gradually. And when it attenuated completely in the soil, the pipeline stopped its response.
4. The peak value of tensile stress of each element of the vault is the largest, followed by that of the bottom plate, and that of the side wall is the smallest. However, the velocity of the bottom plate and the arch roof of pipeline are the largest. The peak values of velocity and tensile stress exist in 0 to 4 m away from the explosion source, and gradually decrease as the distance away from the explosion source increases.

The damage of pipeline under tunnel blasting vibration is mainly governed by the principal tensile stress. However, the velocity is generally monitored to protect the pipeline from the blasting. Therefore, the coupling relationship between the velocity and the

principal stress of pipeline to blasting vibration is supposed to be investigated in the future research.

Acknowledgements This work is supported by the National Natural Science Foundation of China (Project No. 51708317), Key Research and Development Plan of Shandong Province (Project No. 2019GSF111027), the Taishan Scholar Priority Discipline Talent Group program funded by the Shan Dong Province, and first-class discipline project funded by the Education Department of Shandong Province (2019).

References

De A, Morgante AN, Zimmie TF (2016) Numerical and physical modeling of geofom barriers as protection against effects of surface blast on underground tunnels. *Geotext Geomembr* 44(1):1–12

Guan XM, Fu HX, Wang MS, Guo CX, Liu K, Liu TL (2017) Local dynamic response of a masonry structure to the vibrations of tunnel blasting. *Mod Tunn Technol* 54(3):135–141

Guan XM, Zhang L, Wang LM, Fu HX, Yu DM, Chen G, Ding Y, Jiang WL (2019) Blasting vibration characteristics and safety standard of pipeline passed down by tunnel in short distance. *J Cent South Univ (Sci Technol)* 50(11):2870–2885

Hallquist J (2015) LS-DYNA keyword user’s manual R8.0. Livermore Software Technology Corporation, California

Jayasinghe LB, Thambiratnam DP, Perera N, Jayasooriya JHAR (2013) Computer simulation of underground blast response of pile in saturated soil. *Comput Struct* 120:86–95

Jiang JJ, Lu XZ, Ye LP (2005) Finite element analysis of concrete structure. Tsinghua University Press, Beijing

Jiang N, Gao T, Zhou CB, Luo XD (2018) Effect of excavation blasting vibration on adjacent buried gas pipeline in a metro tunnel. *Tunn Undergr Space Technol* 81:590–601

Koneshwaran S (2014) Blast response and sensitivity analysis of segmental tunnel. Queensland University of Technology

Lewis BA (2004) Manual for LS-DYNA soil material model 147. Mathematical models

- Li YC, Shi DY, Zhao Y (2008) Basic theory and engineering practice of ANSYS 110/LS-DYNA. China Water Power Press, Beijing
- Li A, Liu Y, Dai F, Liu K, Wei MD (2020) Continuum analysis of the structurally controlled displacements for large-scale underground caverns in bedded rock masses. *Tunn Undergr Space Technol* 97:103288
- Lin CM, Chen LB, Jiang LL, Zheng HL (2010) Research on blasting stability control technology of large-span highway tunnel with super-small clear spacing at highway expansion project. *Chin J Rock Mech Eng* 29(7):1371–1378
- Liu HB (2012) Soil–structure interaction and failure of cast-iron subway tunnels subjected to medium internal blast loading. *J Perform Constr Facil* 26(5):691–701
- Liu YP, Gong M, Huang GH (2012) Numerical analysis method for optimizing charging structure of deep-hole blasting and its application. *Rock Soil Mech* 33(6):1883–1888
- Liu W, Liu J, Zhu C (2019) Multi-scale effect of acoustic emission characteristics of 3D rock damage. *Arab J Geosci* 12(22):668
- Ma XF, Sui T, Shang JH, Wang DD (2011) Response analysis of dot shield tunnels under internal explosion. *J Tongji Univ* 39(7):983–988
- Malvar LJ, Simons D (1996) Concrete material modeling in explicit computations. In: Workshop on recent advances in computational structural dynamics and high performance computing, USAE waterways experiment station, Vicksburg
- Mane AS, Shete S, Bhuse A (2017) Effect of geofoam inclusion on deformation behavior of buried pipelines in cohesive soils. International congress and exhibition “sustainable civil infrastructures: innovative infrastructure geotechnology”. Springer, Cham
- Mokhtari M, Nia AA (2015) A parametric study on the mechanical performance of buried X65 steel pipelines under subsurface detonation. *Arch Civ Mech Eng* 15(3):668–679
- Mokhtari M, Nia AA (2016) The application of CFRP to strengthen buried steel pipelines against subsurface explosion. *Soil Dyn Earthq Eng* 87:52–62
- Qin Z, Fu HL, Chen XX (2019) A study on altered granite meso-damage mechanisms due to water invasion-water loss cycles. *Environ Earth Sci* 78:428
- Wu N, Liang ZZ, Zhou JR, Zhang YZ (2020) Energy evolution characteristics of coal specimens with preformed holes under uniaxial compression. *Geomech Eng* 20(1):55–66
- Xu HL, Zhang JC, Guo JQ (2003) Investigation on formula of predicting the particle vibration velocity in drilling blasting. *Blasting* 20(3):75–78
- Zhang XH, Duan ZD, Zhang CW (2009) Analysis for dynamic response and failure process of reinforced concrete beam under blast load. *J Northeast For Univ* 37(4):50–53
- Zhang QS, Li LP, Li SC, Ding WT, Hong WL (2008) Experimental study of blasting dynamic vibration of closely adjacent tunnels. *Rock Soil Mech* 29(10):2655–2660
- Zhang K, Zheng QP, Li SW, Hua WX (2013) Numerical simulation & analysis for impact of explosion under ground on buried pipelines. *J Log Eng Univ* 3:12–17
- Zhang L, Liang Z, Zhang J (2016) Mechanical response of a buried pipeline to explosion loading. *J Fail Anal Prev* 16(4):576–582
- Zhang LM, Zhao MS, Chi EA, Huang B, He XG (2017) Experiments for effect of blasting vibration on underground pipeline and risk prediction. *J Vib Shock* 36(16):241–247
- Zhong DW, Huang X, Lu Z, Chen C, Si JF (2018) Experimental study on dynamic response of buried steel tubes with different sizes under blasting loading. *Sci Technol Eng* 18(13):219–223

Publisher's Note Springer Nature remains neutral with regard to jurisdictional claims in published maps and institutional affiliations.